2022 International Symposium on Nonlinear Theory and Its Applications,
NOLTA2022, Virtual, December 12-15, 2022

Detection of Least Acceleration Fluctuation Point of Moving Object by Using Inertial Sensor

Shotaro Ikemoto†, Daisuke Izutsu‡, and Tsuyoshi Mizuguchi⋆

†Department of Mathematical Sciences, Osaka Prefecture University
1–1 Gakuencho, Nakaku, Sakai 599-8531, Japan
‡Department of Physics, Osaka Prefecture University
1–1 Gakuencho, Nakaku, Sakai 599-8531, Japan
⋆ Department of Physics, Osaka Metropolitan University
1–1 Gakuencho, Nakaku, Sakai 599-8531, Japan
Email: gutchi@omu.ac.jp

Abstract—A method is proposed to detect the least shaken point on a moving object to which an inertial sensor is attached by analyzing time series of acceleration and angular velocity measured by the sensor. The calculation procedure is derived and it is applied to the time series obtained from an experiment using a pendulum to estimate the position of the least shaken point. The accuracy of the method is evaluated by comparing it with data obtained by a different method using an image analysis.

1. Introduction

As the recent development of multi-function loggers it becomes easier to obtain multiple data on moving object in various situations, especially in field works. In particular, inertial sensors consisting of accelerometer and gyroscope provide detailed kinematic information that enables us to analyze various behaviors of animals including human[1, 2, 3].

Kinematic characteristics, such as the center of mass, the instantaneous center of rotation, and the zero moment point are important concepts to grasp and/or control the motion of moving body[4, 5]. Estimating such characteristics from the time series of measured acceleration and angular velocity is a kind of an inverse problem. Among a variety of such kinematic characteristics, this study focuses on a point of the smallest fluctuation of acceleration, i.e., the least shaken point on the object. We propose a method to detect this point by combining the time series of acceleration and angular velocity for a given time interval. The identification of this point is expected to provide an insight into the mechanism of motion. Moreover, it also be a candidate location for other sensors, such as optical or acoustic ones, or for a good riding position of a vehicle.

In §2, the main procedure is explained after some definitions and assumptions. In §3, it is applied for real experimental data of a swinging pendulum. Final section is devoted to the discussion.

ORCID iDs S. Ikemoto: 0000-0002-6619-4034, D. Izutsu: 0000-0001-9223-686X, T. Mizuguchi: 0000-0002-5973-4258

2. Least Acceleration Fluctuation Point

The main question is how to find the least shaken point in the object in motion. For example, consider a swinging physical pendulum to which an inertial sensor is attached. We only know the time series of several kinematic quantities such as acceleration and angular velocity. Then how do we estimate the position of the fulcrum of the pendulum by analyzing the time series of these quantities ? In order to answer this question, we calculate the amplitude of acceleration fluctuation at an arbitrary point on the object and find the point where it is minimized.

An inertial sensor S consisting of accelerometer and gyroscope is fixed to a moving object. S measures the acceleration $\vec{A}(t)$ and the angular velocity $\vec{G}(t)$, both of which consist of three components $A_\xi(t), A_\eta(t), A_\zeta(t)$ and $G_\xi(t), G_\eta(t), G_\zeta(t)$. Here, ξ, η and ζ are the three axes fixed to S. The sampling frequency is expressed as $1/\delta t$.

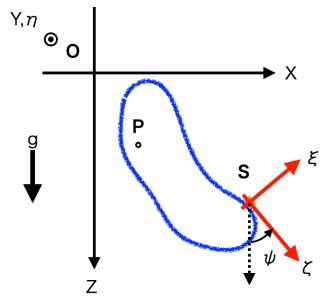

Figure 1: The laboratory coordinates system and the sensor coordinates system in the plane of the object motion, which includes the gravitational vector. O is the origin of LC fixed to somewhere in the laboratory system. S is the sensor and the origin of SC system. P is a point whose coordinates in the SC system are constant in time. ψ (> 0 in this figure) is the angle of SC axes based on the LC axes.

First, we assume that the object motion is limited in a two-dimensional space spanned by the vertical and hori-

zontal axes. In other words, we focus only on the three quantities A_ξ, A_ζ and G_η. And we define a laboratory coordinates system (LC), in which X, Y and Z, where Z axis points the vertically downward and the object moves in the XZ plane. We refer the origin of LC system as O. The positional coordinates of S in LC are (X_S, Y_S, Z_S) with Y_S = const as shown in Fig. 1.

Next, we consider the sensor coordinates system (SC), ξ, η and ζ which is fixed to the sensor. The origin of SC is taken to be the sensor itself. For the simplicity, we assume that the η axis and the Y axis are always parallel. The angle of SC based on LC, ψ, is the elevation angle. If $\psi = 0$, $(A_\xi, A_\eta, A_\zeta) = (0, 0, -g)$ where $g > 0$ is the gravitational acceleration. G_η denotes the angular velocity component around η axis, therefore $G_\eta = \dot{\psi}$ holds.

Now we focus on an arbitrary point P in the XZ plane on the object whose positional coordinates are (ξ_P, ζ_P) in SC and (X_P, Z_P) in LC. We also assume that ξ_P and ζ_P are constants in time. Then the equality $\overrightarrow{OP} = \overrightarrow{OS} + \overrightarrow{SP}$ is written as

$$\begin{pmatrix} X_P \\ Z_P \end{pmatrix} = \begin{pmatrix} X_S \\ Z_S \end{pmatrix} + R(-\psi) \begin{pmatrix} \xi_P \\ \zeta_P \end{pmatrix}, \tag{1}$$

where $R(\psi)$ is a two-dimensional rotation matrix,

$$R(\psi) \equiv \begin{pmatrix} \cos\psi & -\sin\psi \\ \sin\psi & \cos\psi \end{pmatrix}. \tag{2}$$

By considering that ξ_P and ζ_P are constant in time, a following equation is obtained by differentiating Eq.(1) twice:

$$\begin{pmatrix} \ddot{X}_P \\ \ddot{Z}_P \end{pmatrix} = \begin{pmatrix} \ddot{X}_S \\ \ddot{Z}_S \end{pmatrix} + \begin{pmatrix} \Psi_{11} & \Psi_{12} \\ \Psi_{21} & \Psi_{22} \end{pmatrix} \begin{pmatrix} \xi_P \\ \zeta_P \end{pmatrix}, \tag{3}$$

where Ψ_{ij} is given by

$$\begin{aligned} \Psi_{11} = \Psi_{22} &= -\ddot{\psi}\sin\psi - \dot{\psi}^2\cos\psi, \\ \Psi_{12} = -\Psi_{21} &= \ddot{\psi}\cos\psi - \dot{\psi}^2\sin\psi. \end{aligned} \tag{4}$$

Equation (3) gives a relation between the acceleration at the sensor ${}^t(\ddot{X}_S, \ddot{Z}_S)$ and that at the arbitrary point P ${}^t(\ddot{X}_P, \ddot{Z}_P)$. Because the measured acceleration (A_ξ, A_ζ) is with respect to SC, the acceleration of S in LC is given by following equation:

$$\begin{pmatrix} \ddot{X}_S \\ \ddot{Z}_S \end{pmatrix} = R(-\psi) \begin{pmatrix} A_\xi \\ A_\zeta \end{pmatrix} + \begin{pmatrix} 0 \\ g \end{pmatrix}. \tag{5}$$

Now we consider a time series of three quantities $A_\xi(t)$, $A_\zeta(t)$ and $\psi(t)$ of a certain time interval $t_0 < t < t_0 + \tau$. Where is the least shaken point of the object during this interval? In order to specify this point we calculate the amplitude of acceleration fluctuation during the interval at P. The sum of the statistical variance of $\ddot{X}_P$ and $\ddot{Z}_P$ are given by

$$b(\xi_P, \zeta_P) \equiv \langle (\ddot{X}_P - \langle \ddot{X}_P \rangle)^2 \rangle + \langle (\ddot{Z}_P - \langle \ddot{Z}_P \rangle)^2 \rangle, \tag{6}$$

where $\langle\ \rangle$ denotes a temporal average during τ, i.e., $\langle Q \rangle \equiv \frac{1}{\tau}\int_{t_0}^{t_0+\tau} Q dt$ or its discretized version. The lower the value b, the smaller the amplitude of the acceleration fluctuation at that point. And if $b(\xi_P, \zeta_P) = 0$, the acceleration at P does not fluctuate in time during τ.

By substituting Eqs. (3) and (4) into (6), and we omit the subscript P for the simplicity, tedious calculations[6] show that

$$b(\xi, \zeta) = B_2(\xi^2 + \zeta^2) + 2B_{1\xi}\xi + 2B_{1\zeta}\zeta + B_0, \tag{7}$$

with

$$\begin{aligned} B_2 &= \langle (\ddot{\psi})^2 + (\dot{\psi})^4 \rangle - \langle \Psi_{11} \rangle^2 - \langle \Psi_{21} \rangle^2 \\ B_{1\xi} &= \langle \Psi_{11}\ddot{X}_S + \Psi_{21}\ddot{Z}_S \rangle - \langle \Psi_{11} \rangle \langle \ddot{X}_S \rangle - \langle \Psi_{21} \rangle \langle \ddot{Z}_S \rangle \\ B_{1\zeta} &= \langle \Psi_{12}\ddot{X}_S + \Psi_{22}\ddot{Z}_S \rangle - \langle \Psi_{12} \rangle \langle \ddot{X}_S \rangle - \langle \Psi_{22} \rangle \langle \ddot{Z}_S \rangle \\ B_0 &= \langle \ddot{X}_S^2 + \ddot{Z}_S^2 \rangle - \langle \ddot{X}_S \rangle^2 - \langle \ddot{Z}_S \rangle^2. \end{aligned} \tag{8}$$

Equation (7) means that $b(\xi, \zeta)$ takes the minimum value b_* at (ξ_*, ζ_*), with

$$(\xi_*, \zeta_*) = \left(-\frac{B_{1\xi}}{B_2}, -\frac{B_{1\zeta}}{B_2} \right), \tag{9}$$

and

$$b_* = B_0 - \frac{B_{1\xi}^2 + B_{1\zeta}^2}{B_2}. \tag{10}$$

Equation (9) gives the position of point at which the amplitude fluctuation of acceleration in LC takes the minimum value for the given time series between t_0 and $t_0 + \tau$. We refer this point as a least acceleration fluctuation point (LAFP) and Eq. (10) expresses the amplitude of acceleration fluctuation at LAFP.

In order to apply the method described above to a discrete time series of $A_\xi(t_j)$, $A_\zeta(t_j)$ and $G_\eta(t_j)$ with $j = 1, \cdots$, obtained from the sensor, we take a following procedure. First, $\psi(t_j)$ is calculated from $G_\eta(t_j) = \dot{\psi}(t_j)$ by a numerical integration,

$$\psi(t_j) = \psi(t_0) + \sum_{i=0}^{j} G_\eta(t_i)\delta t. \tag{11}$$

Similarly the angular acceleration $\ddot{\psi}(t_j)$ is calculated by a numerical differentiation,

$$\ddot{\psi}(t_j) = \frac{G_\eta(t_{j+1}) - G_\eta(t_j)}{\delta t}. \tag{12}$$

Higher-order corrections to these differentiation / integration are expected to improve the accuracy. $\ddot{X}_S, \ddot{Z}_S$ and Ψ_{ij} with $i, j = 1, 2$ are obtained by Eqs. (4) and (5). Finally the position and the fluctuation amplitude of acceleration of LAFP can be estimated by Eqs. (9) and (10) with substituting all the quantities into Eq. (8).

There are two comments: (i) The initial angle $\psi(t_0)$ does not appear in LAFP position (ξ_*, ζ_*) and the fluctuation amplitude $\sqrt{b_*}$. This is because $\psi(t_0)$ determines the angle

between SC and LC while we focus only on LAFP in the relative position expressed in SC. Mathematically, this can be proofed by showing that $b(\xi, \zeta)$, i.e., all the coefficients B_2, $B_{1\xi}$, $B_{1\zeta}$ and B_0 are invariant under the constant rotation around S, $\psi \to \psi + \text{const}$. Similarly the constant term in Eq. (5), such as g, does not affect the final result on the LAFP position shown in Eq. (9). If we want know the LAFP position in LC, both $\psi(t_0)$ and g should be specified. (ii) No periodicity of ψ, A_ξ, A_ζ is required. In principle, the procedure described above can be applied for an arbitrary τ. It becomes, however, less accurate for too short τ. If so, ψ and $\ddot{\psi}$ become noisy because we obtained these quantities by numerical integration / differentiation of $\dot{\psi} = G_\eta$.

3. Example of swinging pendulum

An experiment using a pendulum with a multi-logger are performed to validate the accuracy of the proposed method. By applying method to the measured time series of acceleration and angular velocity, the position of LAFP is estimated and compared with the result obtained by a different method using image analysis.

The multi-logger is NinjaScan-Light (Switch Science Ltd.) which contains the inertial sensor composed of a tri-axial accelerometer and a tri-axial gyroscope (MPU-6000, TDK InvenSense, sampling frequency 100Hz). This logger is attached to a pendulum (Chaotic Pendulum Ltd.). The pendulum can swing freely around the fulcrum. Therefore LAFP corresponds to the fulcrum in this setup.

Experimental procedure is as follows: Attach the logger to the pendulum. Take several photos of the apparatus with a digital camera, which are used for image analysis described later. Then, let the pendulum swing freely from a certain initial condition for several periods. This procedure is repeated several times with different initial conditions of swing amplitude. Two different setups of the position and the angle of the sensor are performed. When all the procedure is completed, the recorded data are transferred to the computer and converted by dedicated software (`NinjaScan_GUI.exe`) and analyzed by the proposed method.

Figure 2 shows a setup (top), a close up of the logger (inset) and a typical time series obtained from the inertial sensor (bottom). The proposed method is applied to approximately one swing period of time series. Hereafter, the estimated distance and angle from the sensor to LAFP are referred as $l_* \equiv \sqrt{\xi_*^2 + \zeta_*^2}$ and $\phi_* \equiv \tan^{-1}(\zeta_*/\xi_*)$, respectively.

Apart from this procedure, the distance and the angle from the sensor to the fulcrum are measured by the image analysis of the apparatus. Namely, a pair of markers is attached to the logger to specify the position and the direction of axis of the sensor (Fig 2). Several still images with different swing angles of the pendulum are taken by a digital camera for each setup and analyzed by ImageJ[7]. The positions of the markers are measured in each image. Then

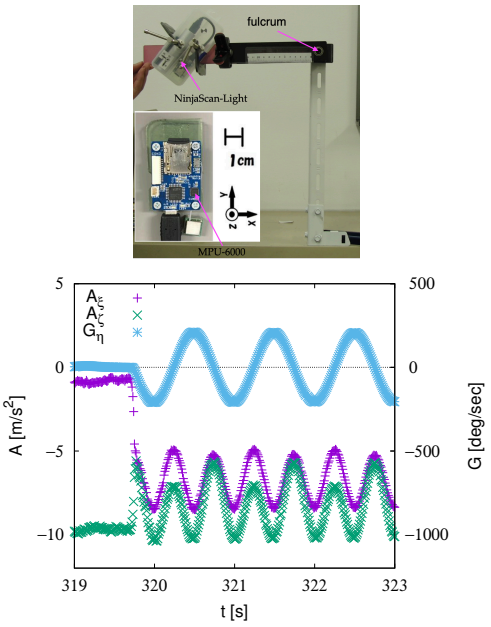

Figure 2: (top) The experimental setup. The inertial sensor (NinjaScan-Light) is attached to the pendulum. The time series of acceleration and angular velocity are recorded in a micro SD card. After trials of the pendulum swinging, data in the micro SD card are transferred to PC and analyzed. A close up of the logger is shown in the inset. Apart from the proposed method, the fulcrum position relative to the sensor is measured by an image analysis. The distance between the sensor and the fulcrum is 0.26 m in this setup. (bottom) Typical time series of acceleration and angular velocity. The pendulum starts to swing at $t \approx 319.8$ s, whose period is approximately 1 s. In this case the both A_ξ and A_ζ have two peaks in a period. This is because the sensor is attached to the pendulum at an angle.

the position of the fulcrum is estimated as an equi-distance point from the same marker in different images. The distance between the estimated position of fulcrum and the sensor marker by the image analysis is referred as l_F. The angle between the ξ axis and the vector from the sensor to the fulcrum is ϕ_F.

Figure 3 is the result of comparison of (a) the length (l_F and l_*) and (b) the angle (ϕ_F and ϕ_*). If the points lay on the diagonal line, it means that there are no errors. There are six data, i.e., two setups with different position and angle of the sensor, and three different swinging amplitudes for each setup. All of them lay near the diagonal line as shown in Fig. 3. The error are estimated as $|l_F - l_*| < 3 \times 10^{-3}$ [m] and $|\phi_F - \phi_*| < 1.5$ [deg] for these setups.

In this analysis, we exhibit the result using the time series of A_ξ, A_ζ and G_η of almost one swing period ($\approx$ 1 s) from a certain timing. As noted in the end of the previous section, the result is not changed qualitatively unless too short interval of time series is used.

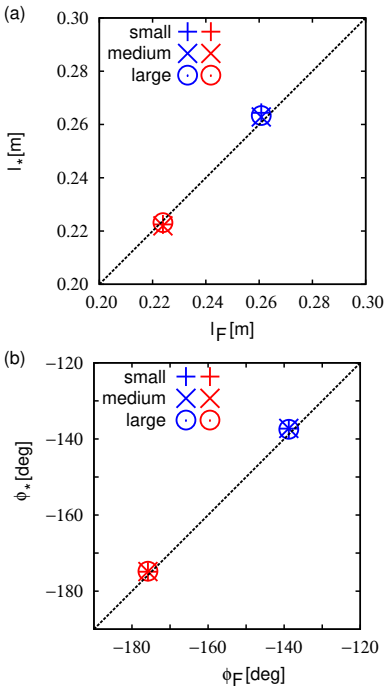

Figure 3: Validation of the method, the distance (a) and the angle (b) from the sensor to LAFP. In both plots, the horizontal and the vertical axes correspond to the measured values from the image analysis and the estimated value from the proposed method, respectively. Two setups with different l and ϕ are shown by different colors, i.e., $(l_F, \phi_F) \approx (0.224, -175.8)$ [m,deg] (red) and $(0.261, -138.8)$ [m, deg] (blue). For each setup, three trials with different swing amplitude are shown by different symbols, i.e., $\sim$ 5 deg (small), $\sim$ 20 deg (medium) and $\sim$ 80 deg (large). All of them lay near the diagonal line which means no errors.

4. Summary

The proposed method estimates the position of LAFP, i.e., the least shaken point on the object, from the time series of acceleration and angular velocity obtained by an inertial sensor attached to the object in motion. The position of LAFP is compared by the image analysis method for a pendulum experiment. Unlike the image analysis method, the advantage of not requiring to measure from outside and the smallness of the error both demonstrate the usefulness of the proposed method. In order to evaluated the accuracy in different situations, positional tracking system based on image analysis such as OpenPose may be applicable[8]. From the time series of positional data, the acceleration and its fluctuation of focused points may be estimated.

A possible significance of LAFP is that it may characterize the qualitatively different motions of animal locomotion. For example, the location of the LAFP in human gait, i.e., walking and running and their relationship to the form of locomotion may be considered[9]. Another significance is its application as an index for determining the comfortable place to ride in a vehicle. According to ISO 2631-1, the effective value of vibration acceleration of whole body vibration is used to evaluate ride comfort[10]. By Applying a frequency filter, it can be useful to find the most comfortable place to ride.

In this analysis, the motion of the object is limited to the two-dimensional vertical plane. In case of animal locomotion, this is valid for a symmetrical motion with respect to the sagittal plane. There are, however, many gaits or three-dimensional maneuvers which do not hold this symmetry. In these cases, an extension to the three-dimensional motion is required. The quartanion formula is promising.

Acknowledgments

The authors would like to thank Professor T. Hoirta for valuable comments.

References

[1] Y. Ohtaki, K. Sagawa, and H. Inooka, "A Method for Gait Analysis in Daily Living Environment by Body-Mounted Instruments," *JSME Int. J. C*, vol.44, pp.1125–1132, 2001; A. M. Sabatini, et al., "Assessment of Walking Features From Foot Inertial Sensing," *IEEE Trans. Biomed. Eng.*, vol.52, pp.486–494, 2005.

[2] L. Gerencsér, et al., "Identification of Behaviour in Freely Moving Dogs (*Canis familiaris*) Using Inertial Sensors," *PLoS ONE*, vol.8, e77814-1–14, 2013.

[3] E. Dorschky, et al., "Estimation of gait kinematics and kinetics from inertial sensor data using optimal control of musculoskeletal models," *J. Biomech.*, vol.95, pp.109278-1–9, 2019.

[4] R. S. Hartenberg, J. Denavit, *Kinematic Synthesis of Linkages*, McGraw-Hill, New York, 1964.

[5] M. Vukobratović, B. Borovac, "Zero-moment point — Thirty five years of its life," *Int. J. Humanoid Robotics*, vol.1, pp.157–173, 2004.

[6] T. Mizuguchi, private communication, 2022.

[7] A public domain Java image processing program. See `https://imagej.nih.gov/ij/`.

[8] Z. Cao, et al., "Realtime Multi-person 2D Pose Estimation Using Part Affinity Fields," *2017 IEEE Conference on Computer Vision and Pattern Recognition (CVPR)*, pp. 1302–1310, 2017.

[9] S. Ikemoto, D. Izutsu, and T. Mizuguchi, in preparation.

[10] International Organization for Standardization, "Mechanical vibration and shock — Evaluation of human exposure to whole-body vibration — Part 1: General requirements," *ISO*, 2631-1, 1997.